PHYSICAL REVIEW D VOLUME 23, NUMBER 12 15 JUNE 1981

# Hamiltonian calculations for the $Z_2$ lattice gauge theory with matter fields

Jay L. Banks
*Department of Physics, Ohio State University, Columbus, Ohio 43210*

D. K. Sinclair
*Department of Physics, University of Illinois at Urbana-Champaign, Urbana, Illinois 61801*
(Received 2 February 1981)

We study the $Z_2$ lattice gauge theory coupled to scalar matter fields (Ising spins) in $2+1$ dimensions. Strong-coupling expansions are obtained for the masses of both "meson" and "glueball" excitations. We use the zeros of the mass gap, obtained using Padé approximants and duality transformations, to locate second-order phase transitions as a function of the gauge and matter coupling constants. The resulting phase diagram is in reasonable agreement with that obtained by other methods. These other methods (Monte Carlo and $1/N$ expansions) are, however, most sensitive to first-order phase transitions while our method is most sensitive to continuous phase transitions. We observe that the additional parameter of the Hamiltonian approach is essentially irrelevant.

Lattice gauge theories including dynamical matter fields have attracted a great deal of interest in recent years.[1-5] Such theories are clearly relevant to the problem of quark confinement, since studies of the confinement question in the context of "pure" gauge theories can only deal with the potential between static sources. If we hope to gain a realistic understanding of confinement, and other features of the spectrum, in a universe which contains quarks as well as gluons, then we must study models whose Lagrangians contain matter as well as gauge fields.

Unfortunately, the model which seems most realistic for the strong interactions—SU(3) gauge theory coupled to fermions—has to date not proven amenable to a thorough treatment of the confinement problem. Although substantial progress has been made towards understanding confinement in the pure gauge theory,[6] the results with fermions have been rather indecisive up to the present.[7] We are thus led to consider simplified models. The particular simplifications made in the present work are to consider a discrete, Abelian gauge group (in this case $Z_2$) and, more importantly for the tractability of the model, to couple the gauge theory to scalar, rather than fermion, matter fields.

Previous treatments of the $Z_2$ "gauge-Higgs" theory[1,2,4] have considered the partition function

$$Z=\sum_{\sigma,\rho=\pm1}\exp\left(\kappa\sum_{\vec{r},\mu\nu}\sigma(\vec{r},\hat{\mu})\sigma(\vec{r}+\hat{\mu},\hat{\nu})\sigma(\vec{r}+\hat{\mu}+\hat{\nu},-\hat{\mu})\sigma(\vec{r}+\hat{\nu},-\hat{\nu})+\beta\sum_{\vec{r},\mu}\rho(\vec{r})\sigma(\vec{r},\hat{\mu})\rho(\vec{r}+\hat{\mu})\right). \tag{1}$$

Here $\sigma(\vec{r},\hat{\mu})$ is a gauge field defined on links $(\vec{r},\hat{\mu})$ and $\rho(\vec{r})$ is a scalar matter field (Ising spin) defined at sites $\vec{r}$ of a cubic lattice in $d+1$ dimensions, where we restrict ourselves to the case $d+1=3$. Each $\sigma$ and each $\rho$ take the values $\pm1$. The two terms in the exponent of Eq. (1) are lattice analogs of $F_{\mu\nu}^2$ and the gauge-covariant derivative terms, respectively, in gauge-invariant continuum theories. The partition function (1) is invariant under changing of the sign of $\rho$ at any given site and simultaneously changing that of the $\sigma$'s on the $2(d+1)$ links emanating from that site. A general gauge transformation is the composition of any number of such site transformations.

Fradkin and Shenker[1] have elucidated the general structure of the phase diagram of the model of Eq. (1). Firstly, the model simplifies for $\beta\to0$ and also for $\kappa\to\infty$. In the former case, the matter field decouples, and we are left with the pure gauge theory first discussed by Wegner[8] which is dual to the Ising model. In the latter limit, the gauge field is "frozen" at $\sigma=1$ (up to gauge transformations) and the interaction of the matter field is that of the ordinary Ising model. In addition, it can be shown[8] that the phase transitions of these limit models persist along lines extending into the $\beta$-$\kappa$ plane; these lines tend to smaller $\kappa$ as $\beta$ increases from zero, and to larger $\beta$ as $\kappa$ decreases from infinity, respectively. (N.B., the model also simplifies for $\kappa\to0$ to the trivially soluble annealed spin-glass model.)

The most interesting result of Fradkin and Shenker holds if the matter fields are in the fundamental representation of the gauge group (for $Z_2$ the only nontrivial representation). In this case, there is a region of nonzero width along the $\kappa=0$ and

 

$\beta=\infty$ edges of the phase diagram where the free energy is analytic.[1] This region connects the "confining" phase of the pure gauge theory (the disordered phase of the Ising theory to which it is dual) to the magnetized phase of the pure spin model. This means that the analogs of quark confinement and of the Higgs mechanism occur in the same phase of the system.[1]

We have studied this model in the Hamiltonian formulation. By standard methods involving the transfer matrix and time continuum limit,[9] we obtain the Hamiltonian

$$H=-\tfrac{1}{2}\sum_{l}(\sigma_1-1)-\tfrac{1}{2}\eta\sum_{i}(\rho_1-1)$$
$$-x\sum_{p}\sigma_3\sigma_3\sigma_3\sigma_3-\xi x\sum_{l}\rho_3\sigma_3\rho_3 \qquad (2)$$

for a quantum system on a two-dimensional spatial lattice. Here $i$ labels sites, $l$ links, and $p$ plaquettes. The $\rho$'s and $\sigma$'s are sets of independent Pauli spin matrices on the sites and links, respectively.

This Hamiltonian is invariant under an arbitrary product of single-site gauge transformations, each of which involves flipping $\rho_3$ at a given site and $\sigma_3$ on each of the four links connected to it. Such a transformation is produced by the operator

$$G(\vec{r})=\rho_1(\vec{r})\sum_{i=1}^{4}\sigma_1(\vec{r},i)\,, \qquad (3)$$

where the product is over the $\pm x$ and $\pm y$ directions. $G(\vec{r})$ clearly commutes with $H$.

We note that $H$ of Eq. (2) depends on three parameters compared with the two of the partition function Eq. (1). This occurs because the Hamiltonian derives from the partition function for an anisotropic lattice, which has four coupling constants instead of two. One is absorbed into the Hamiltonian normalization, but three survive.

Our detailed study of this model starts in the "strong-coupling" regime, where $x$ is small and $\xi$ is finite. We now perturb around $x=0$. The zeroth-order Hamiltonian is

$$H_0=-\tfrac{1}{2}\sum_{l}(\sigma_1-1)-\tfrac{1}{2}\eta\sum_{i}(\rho_1-1)\,. \qquad (4a)$$

The perturbation is

$$V=-x\sum_{p}\sigma_3\sigma_3\sigma_3\sigma_3-\xi x\sum_{l}\rho_3\sigma_3\rho_3\,. \qquad (4b)$$

The zeroth-order ground state is thus an eigenstate of all $\sigma_1$'s and $\rho_1$'s with eigenvalue +1 for each. This state is clearly gauge invariant [see Eq. (3)]. Excitations above this state involve "flipping" spins on various sites and/or links, at a cost of zeroth-order energy $E_\sigma=1$ per flipped $\sigma_1$ and $E_\rho=\eta$ per flipped $\rho_1$. To maintain gauge invariance requires either closed loops of flipped $\sigma_1$'s or "strings" of flipped $\sigma_1$'s with flipped $\rho_1$'s at each end. The lowest-lying zeroth-order gauge-invariant excitations are thus (1) a "boxiton" of four flipped $\sigma_1$'s forming a plaquette, and (2) a "meson" or link excitation of flipped $\rho_1$'s on two adjacent sites, joined by a flipped $\sigma_1$. These states have the zeroth-order energies:

$$E^{(0)}_{\text{vac}}=0\,,\quad E^{(0)}_{\text{box}}=4\,,\quad E^{(0)}_{\text{link}}=1+2\eta\,, \qquad (5)$$

respectively.

We have used Rayleigh-Schrödinger perturbation theory to expand the energies of these excited states to order $x^4$. The graphs contributing at order $x^2$ to $E_{\text{link}}$ and $E_{\text{box}}$ are given in Figs. 1 and 2, respectively. Their values are listed in Table I. The calculations are similar in principle, but considerably more complicated and tedious in detail, for third and fourth orders. The results are

$$E_{\text{link}}-E_{\text{vac}}=l_{00}+(l_{20}+l_{22}\xi^2)x^2+l_{32}\xi^2x^3$$
$$+(l_{40}+l_{42}\xi^2+l_{44}\xi^4)x^4+O(x^5)\,, \qquad (6a)$$

$$E_{\text{box}}-E_{\text{vac}}=b_{00}+(b_{20}+b_{22}\xi^2)x^2$$
$$+(b_{40}+b_{42}\xi^2+b_{44}\xi^4)x^4+O(x^5)\,, \qquad (6b)$$

where the coefficients are given in Table II as functions of $\eta$.

Although we have calculated both the boxiton and the link series for all $\eta$, what we really want is the lowest-lying excitation. This is the meson for $\eta<\frac{3}{2}$ and the boxiton for $\eta>\frac{3}{2}$.

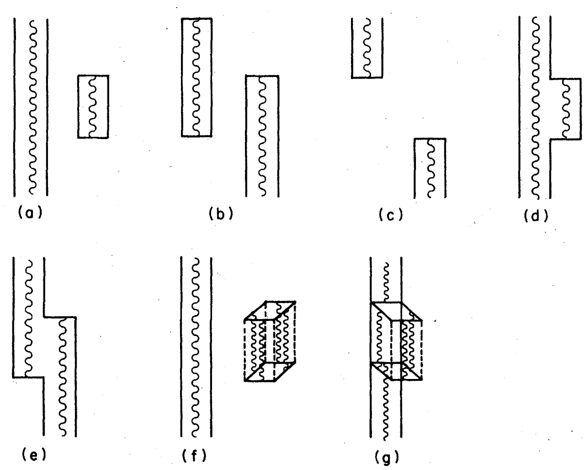


FIG. 1. Graphs giving the second-order contribution to the meson or link energy. Solid lines represent flipped spins, wavy lines represent links on which the gauge field is excited.

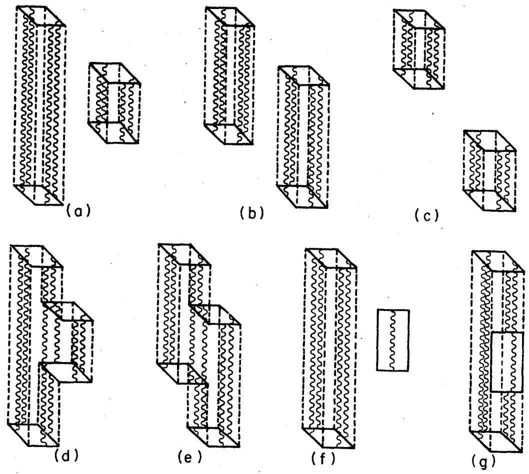


FIG. 2. Graphs giving the second-order contribution to the boxiton energy.

The signal for second-order phase transitions in this model is the vanishing of the "mass gap" as given by Eq. (6a) if $\eta < \frac{3}{2}$ and Eq. (6b) if $\eta > \frac{3}{2}$, on a surface in $x-\xi-\eta$ space. We use [2, 2] Padé approximants (in the variable $x$) to analytically continue the series of Eq. (6) outside the small-$x$ domain. The real positive zeros of the approximants give us our estimate of the zeros of the mass gap, and hence the position of the second-order phase transitions in the theory.

Further information concerning the positions of the second-order phase transitions of the theory can be obtained using the self-duality of the theory. This is far from transparent in the $x-\eta-\xi$ variables[10] so we transform to a new set of variables $z-\lambda-\mu$ given by

$$z=\left(\frac{2\xi x}{\eta}\right)^{1/2}, \tag{7a}$$

$$\lambda=\frac{1}{\sqrt{2x}}, \tag{7b}$$

$$\mu=\sqrt{\eta\xi}. \tag{7c}$$

Then

$$W\equiv\frac{2\lambda}{\mu}H=\frac{\lambda}{\sqrt{\mu}}\sum_{l}(\sigma_1-1)-\frac{\sqrt{\mu}}{z}\sum_{l}(\rho_1-1)$$
$$-\frac{1}{\sqrt{\mu}\lambda}\sum_{p}\sigma_3\sigma_3\sigma_3\sigma_3-\sqrt{\mu}\,z\sum_{l}\rho_3\sigma_3\rho_3.$$

The duality transformation is[3,5]

$$\sigma_1\rightarrow\tilde{\rho}_3\tilde{\sigma}_3\tilde{\rho}_3, \tag{8a}$$

$$\sigma_3\sigma_3\sigma_3\sigma_3\rightarrow\tilde{\rho}_1, \tag{8b}$$

$$\rho_1\rightarrow\tilde{\sigma}_3\tilde{\sigma}_3\tilde{\sigma}_3\tilde{\sigma}_3, \tag{8c}$$

$$\rho_3\sigma_3\rho_3\rightarrow\tilde{\sigma}_1, \tag{8d}$$

where the tilde quantities are again Pauli spin matrices. Thus

$$W(z,\lambda,\mu)\rightarrow W(z^*,\lambda^*,\mu^*),$$

where

$$z^*=\lambda, \tag{9a}$$

$$\lambda^*=z, \tag{9b}$$

$$\mu^*=1/\mu. \tag{9c}$$

Thus a zero at $z=z_0$, $\lambda=\lambda_0$, $\mu=\mu_0$ maps into another at $z=z_0^*$, $\lambda=\lambda_0^*$, $\mu=\mu_0^*$.

Figures 3–5 give our predictions for the lines of zeros of the mass gap and hence of second-order transitions. These three phase diagrams are for $\mu$ of 1, 0.2, and 0.1, respectively. Note that the zeros of Fig. 3 come entirely from the boxiton mass. Duality makes the $\mu=1$ diagram symmetric under interchange of $z$ and $\lambda$. The phase diagrams for $\mu=5$ and 10 are obtained from those for $\mu=0.2$ and $\mu=0.1$ by interchange of $z$ and $\lambda$. In each case the nearly vertical line of zeros is from $W(z,\lambda,\mu)$, the nearly horizontal line from $W(z^*,\lambda^*,\mu^*)$ with $z^*$, $\lambda^*$, and $\mu^*$ given by Eq. (9).

The question immediately arises as to why the lines of zeros obtained from $W(z,\lambda,\mu)$ and $W(z^*,\lambda^*,\mu^*)$ do not coincide and which, if any, of these zeros we believe. For this we turn to previous analyses for the case $\mu=1$.[2-4] These find that, in addition to the lines of second-order transitions which we have found, there exists also a line of first-order transitions extending from the point where these lines of second-order transi-

TABLE I. Values of graphs of Figs. 1 and 2.

| | Fig. 1 | Fig. 2 |
|---|---|---|
| (a) | $\frac{(N-7)\xi^2}{-(1+2\eta)}x^2$ | $\frac{(N/2)-5}{-4}x^2$ |
| (b) | $\frac{(N-7)\xi^2}{-(1+2\eta)}x^2$ | $\frac{(N/2)-5}{-4}x^2$ |
| (c) | $\frac{N\xi^2}{(1+2\eta)}x^2$ | $\frac{N/2}{4}x^2$ |
| (d) | $\frac{6\xi^2}{-1}x^2$ | $\frac{4}{-2}x^2$ |
| (e) | $\frac{6\xi^2}{-1}x^2$ | $\frac{4}{-2}x^2$ |
| (f) | $\frac{(N/2)-2}{-4}x^2$ | $\frac{(N-4)\xi^2}{-(1+2\eta)}x^2$ |
| (g) | $\frac{2}{-2}x^2$ | $\frac{4\xi^2}{-(2\eta-1)}x^2$ |

TABLE II. Coefficients of the strong-coupling expansions for (a) $E_{\text{link}}-E_{\text{vac}}$ and (b) $E_{\text{box}}-E_{\text{vac}}$. In each case the subscript "$ij$" labels the coefficient of $\xi^j x^i$.

| $E_{\text{link}}-E_{\text{vac}}$ | $E_{\text{box}}-E_{\text{vac}}$ |
|---|---|
| $l_{00}=1+2\eta$ | $b_{00}=4$ |
| $l_{20}=-\frac{1}{2}$ | $b_{20}=-\frac{3}{2}$ |
| $l_{22}=-12+14/(1+2\eta)$ | $b_{22}=-8/(4\eta^2-1)$ |
| $l_{32}=-16-4/(1+2\eta)-4/(1+2\eta)^2$ | $b_{40}=\frac{43}{96}$ |
| $l_{40}=-\frac{3}{32}$ | $b_{42}=(18\eta+11)/(2\eta+1)^2+5(2\eta+5)^2/4(2\eta+3)(2\eta+1)^2$ |
| $l_{42}=-(8\eta^3+4\eta^2-18\eta-1)/(2\eta+3)(2\eta+1)^3$ | $+5(2\eta+3)/4(2\eta-1)^2-3(2\eta+3)^2/(2\eta+1)^3-3/(2\eta-1)$ |
| $l_{44}=(576\eta^4+632\eta^3+172\eta^2+128\eta-12)/(\eta+1)(2\eta+1)^3$ | $-(2\eta+1)(6\eta-1)/(2\eta+3)(2\eta-1)^2+(34\eta+83)/2(4\eta^2-1)$ |
| | $-32/(2\eta+1)^2(2\eta-1)^2(2\eta-3)$ |
| | $b_{44}=-(864\eta^4-896\eta^3+424\eta^2+32\eta+8)/(\eta^2-1)(4\eta^2-1)^3$ . |

tions cross, along the self-dual line ($z=\lambda$) out to $z\approx 1.1$ where it terminates. We have sketched this as a line of crosses in Fig. 3. (N.B., the point where this line terminates is outside our range.) Now we see what our problem is. To the low order to which we have calculated, our series are incapable of delineating this line of first-order transitions. Hence any zeros which lie beyond this line are likely to be displaced, which is exactly what we see. This means that we can only trust that part of our lines of zeros prior to the point at which they cross (unbroken lines). Those zeros beyond this point (broken lines) should be ignored and considered as the displaced version of the zeros coming from the dual Hamiltonian. The same analysis should be true for $\mu=0.2$ and $\mu=0.1$.

The fact that the vertical lines of zeros for $\mu=0.2$ and $\mu=0.1$ are discontinuous is because the lower part of the curve comes from the boxiton, while the upper part comes from the link. The discontinuity occurs at $\eta=\frac{3}{2}$ (i.e., $z\lambda=2\mu/3$). If our results were exact, these two curves would match at this point. The fact that they do not is a measure of the reliability of our approximation.

In each case, our lines of zeros isolate the bottom left-hand corner of the phase diagram. This region is to be interpreted as a "free-charge" phase, separated by second-order phase transitions from the other "Higgs-confinement" phase. This is in good agreement with other analyses using Monte Carlo[2,4] methods or $1/N$ expansions.[3] The points of intersection of these phase boundaries with the axes for $\mu=1$, viz., $z\approx 0.37$ and

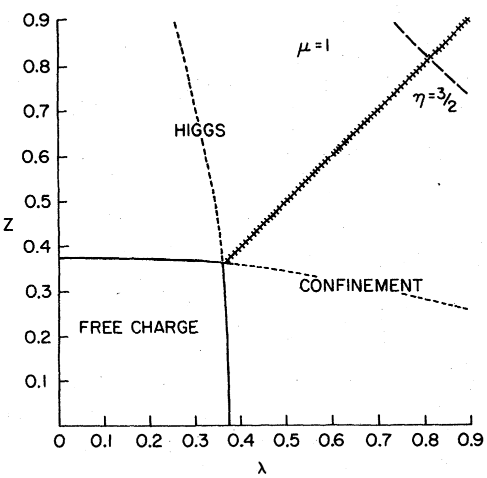


FIG. 3. The phase diagram for $\mu=1$. Solid lines represent second-order phase transitions. The line of crosses indicates first-order phase transitions. The broken lines are displaced zeros of the mass gap.

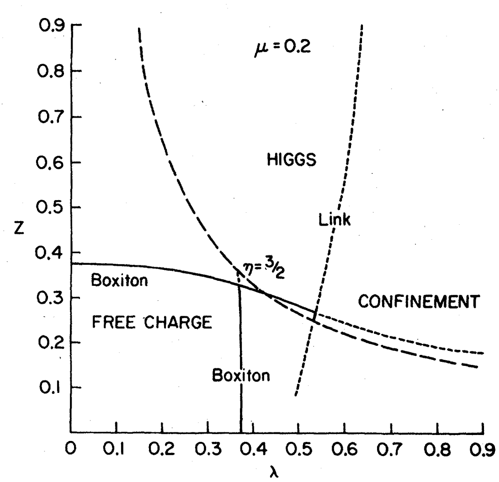


FIG. 4. The phase diagram for $\mu=0.2$. Note the crossover from boxiton to link at $\eta=\frac{3}{2}$. The curve $n^*=\frac{3}{2}$ lies completely outside the plotted range of variables.

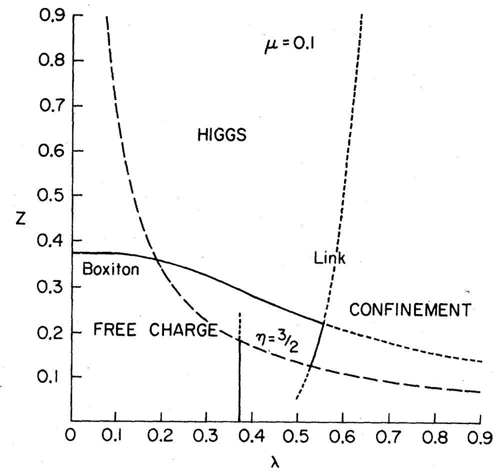


FIG. 5. The phase diagram for $\mu=0.1$. Note the crossover from boxiton to link at $\eta=\frac{3}{2}$. The curve $n^*=\frac{3}{2}$ lies completely outside the plotted range of variables.

$\lambda\approx 0.37$, are in good agreement with the $1/N$ expansion[3] which gives the values $z=0.405$ and $\lambda=0.405$. The direction of curvature of these lines—slightly towards smaller $\lambda(z)$ values rather than towards larger $\lambda(z)$ values—does not agree, however; but it will be noticed that the link zeros for $\mu=0.2$ and $\mu=0.1$ do have this property. This is to be expected since the link series has more terms and is thus probably more reliable than that for the boxiton.

It is expected that higher-order calculations would improve these results and show indications of the line of first-order transitions. This is only possible because the line of first-order transitions terminates, allowing analytic continuation from one side to the other of this line.

The close similarity of our phase diagrams for the large range of $\mu$ investigated $0.1\le\mu\le 10$ would seem to indicate that $\mu$, or some closely related parameter, is irrelevant at or near the critical points of the theory. This would mean that the critical behavior of the theory is described by only two of the three parameters of the theory. We might expect this to happen, since our extra parameter is a result of the anisotropy of the Hamiltonian theory. Such anisotropy would be expected to vanish at a critical point where symmetries are likely to be restored.

To summarize, our calculations of the phase boundaries of the $Z_2$ Abelian Higgs model are in agreement with previous calculations using different methods[1-5] except that we cannot elucidate the first-order transitions to this low order.

At this point we should emphasize that the advantage of our method lies in that these analytic techniques are most suited for finding zeros in functions where the zero is approached continuously. It is thus most suited to finding continuous phase transitions. Monte Carlo techniques, on the other hand, are numerical in nature and are thus most suited to finding the abrupt discontinuities associated with first-order transitions. $1/N$ expansions are also best suited to finding first-order transitions.

Finally we should point out that the results of Table II represent, as far as we know, the only explicit calculation of the low-lying excitation spectrum of this model.

The authors wish to thank J.B. Kogut for many stimulating conversations and assistance with the programming. In addition we thank Professor R.F. Dashen for hospitality at the Institute for Advanced Study, where some of this work was performed. One of us (J.L.B.) would also like to thank Dennis Kane and the directors and staff of the computer-based Education Research Laboratory, University of Illinois, for the use of the University's PLATO computer system, on which an earlier version of the calculations were performed. The algebra and series manipulations leading to the figures and curves presented here were obtained from MACSYMA which is supported by the U.S. Energy Research and Development Administration under Contract No. E(11-1)-30-70 and by NASA under Grant No. NSG-13-23. The work of J.L.B. was supported in part by the National Science Foundation under Grant No. NSF PHY-79-00272 while a summer research student at the University of Illinois.

---

[1]E. Fradkin and S. Shenker, Phys. Rev. D 19, 3682 (1979).

[2]M. Creutz, Phys. Rev. D 21, 1006 (1980).

[3]R. J. Elliot and P. Pfeuty, J. Phys. C 4, 2370 (1971); J. B. Kogut, Phys. Rev. D 21, 2316 (1980).

[4]G. A. Jongeward, J. D. Stack, and C. Jayaprakash, Phys. Rev. D 21, 3360 (1980).

[5]D. Horn and E. Katznelson, Phys. Lett. 91B, 397 (1980).

[6]J. B. Kogut, R. B. Pearson, and J. Shigemitsu, Phys. Rev. Lett. 43, 484 (1979); M. Creutz, Phys. Rev. D 21, 2308 (1980).

[7]T. Banks, S. Raby, L. Susskind, J. Kogut, D. R. T. Jones, P. N. Scharbach, and D. K. Sinclair, Phys. Rev. D 15, 1111 (1977).

[8]F. Wegner, J. Math. Phys. 12, 2259 (1971).

[9]J. B. Kogut and L. Susskind, Phys. Rev. D 11, 395 (1975); J. B. Kogut, Rev. Mod. Phys. 51, 659 (1979).

[10]D. K. Sinclair (unpublished); J. L. Banks, Ph.D. thesis, Cornell University, 1980 (unpublished).